Journal of Inorganic Biochemistry 198 (2019) 110752

Contents lists available at ScienceDirect

Journal of Inorganic Biochemistry

journal homepage: www.elsevier.com/locate/jinorgbio

Systematic investigation of the antiproliferative activity of a series of ruthenium terpyridine complexes

Johannes Karges[a], Olivier Blacque[b], Marta Jakubaszek[a,c], Bruno Goud[c], Philippe Goldner[d], Gilles Gasser[a,*]

[a] Chimie ParisTech, PSL University, CNRS, Institute of Chemistry for Life and Health Sciences, Laboratory for Inorganic Chemical Biology, 75005 Paris, France
[b] Department of Chemistry, University of Zurich, Winterthurerstrasse 190, 8057 Zurich, Switzerland
[c] Institut Curie, PSL University, CNRS UMR 144, Paris, France
[d] Chimie ParisTech, PSL University, CNRS, Institut de Recherche de Chimie Paris, 75005 Paris, France

ARTICLE INFO

Keywords:
Anticancer
Medicinal inorganic chemistry
Metals in medicine
Photodynamic therapy
Ruthenium

ABSTRACT

Due to acquired resistance or limitations of the currently approved drugs against cancer, there is an urgent need for the development of new classes of compounds. Among others, there is an increasing attention towards the use of Ru(II) polypyridyl complexes. Most studies in the literature were made on complexes based on the coordination of N-donating bidentate ligands to the ruthenium core whereas studies on 2,2′:6′, 2″-terpyridine (terpy) coordinating ligands are relatively scare. However, several studies have shown that $[Ru(terpy)2]^{2+}$ derivatives are able bind to DNA through various binding modes making these compounds potentially suitable as chemotherapeutic agents. Additionally, light irradiation of these compounds was shown to enable DNA cleavage, highlighting their potential use as photosensitizers (PSs) for photodynamic therapy (PDT). In this work, we present the systematic investigation of the potential of 7 complexes of the type [Ru(terpy)(terpy-X)]2+ (X = H (**1**), Cl (**2**), Br (**3**), OMe (**4**), COOH (**5**), COOMe (**6**), NMe2 (**7**)) as potential chemotherapeutic agents and PDT PSs. Importantly, six of the seven complexes were found to be stable in human plasma as well as photostable in acetonitrile upon continuous light irradiation (480 nm). The determination of the distribution coefficient log*P* values for the **7** complexes revealed their good water solubility. Complex **7** was found to be cytotoxic in the micromolar range in the dark as well as to have some phototoxicity upon light exposure at 480 nm in non-cancerous retinal pigment epithelium (RPE-1) and cancerous human cervical carcinoma (HeLa) cells.

Synopsis: The systematic investigation of the potential of 7 complexes of the type $[Ru(terpy)(terpy-X)]^{2+}$ (terpy: 2,2′:6′, 2″-terpyridine; X = H (**1**), Cl (**2**), Br (**3**), OMe (**4**), COOH (**5**), COOMe (**6**), NMe2 (**7**)) as potential chemotherapeutic agents and photosensitizers for photodynamic therapy is presented.

1. Introduction

Based on the increasing impact of cancer on the life quality as well as mortality in the world, research efforts are made towards the development of new methods for the treatment of this disease as well as the improvement of existing anticancer drugs. Most commonly, cancer is fought through the combination of different techniques (i.e. chemotherapy, surgery, radiotherapy and immunotherapy) [1–3]. To date, the gold standard in the chemotherapeutic treatment of cancer is the platinum drug cisplatin and its derivatives carboplatin and oxaliplatin [4,5]. However, although the ability of cisplatin for the treatment of patients with cancer is impressive and undeniable, treatments with this drug are also associated with severe side effects that include nerve and kidney damage, nausea, vomiting and bone marrow suppression. Acquired resistances limit also the use of cisplatin and its derivatives these derivatives. These drawbacks have led, in the last decades, to the search for alternative compounds and, among others, of non-platinum based compounds. Among the new classes investigated, coordinatively saturated, inert Ru(II) polypyridyl complexes are receiving increasing attention due to their promising anticancer and antimicrobial activity as chemotherapeutic agents as well as photodynamic therapy (PDT) photosensitizers (PSs) [6–17]. Very importantly, one of Mc Farland and coworkers' ruthenium-based PDT PSs, namely TLD-1433, just completed phase I clinical trial as a PDT PS against bladder cancer [10].

* Corresponding author.
E-mail address: gilles.gasser@chimieparistech.psl.eu (G. Gasser).
URL: https://www.gassergroup.com/ (G. Gasser).

https://doi.org/10.1016/j.jinorgbio.2019.110752
Received 1 February 2019; Received in revised form 8 June 2019; Accepted 14 June 2019
Available online 17 June 2019
0162-0134/

In the field of ruthenium-based PDT PSs, most studies in the literature are based on a $[Ru(bipy/phen/bphen/dppz)_3]^{2+}$ (bipy = 2,2′-bipyridine, phen = 1,10-phenanthroline, bphen = 4,7-diphenyl-1,10-phenanthroline, dppz = dipyrido[3,2-a:2′,3′-c]phenazine) scaffold due to their interesting redox properties, long excited-state lifetimes as well as intense luminescence [11,13,18–24]. In comparison, complexes based on a $[Ru(terpy)_2]^{2+}$ (terpy = 2,2′:6′, 2″-terpyridine) scaffold have not been very extensively studied. These complexes are well-known to have a short-lived excited state and to be weakly luminescent at room temperature but long-lived and strongly luminescent at low temperature (77 K). This phenomenon is explained by an unfavourable bite angle of the ligands for the octahedral coordination of the Ru(II). As a result, a relatively low ligand field state ^{3}LF (ligand-field) is created which is able to quench the normally emitting ^{3}MLCT (metal-to-ligand charge-transfer) state [20,25]. Despite these unfavourable photophysical properties, several studies have shown that these complexes were still able to bind to DNA and to cleave it upon light irradiation, making them potential PSs for PDT purposes [26–30]. Interestingly, it was demonstrated that these complexes were able to interact in different manners with DNA, including electrostatic interactions, intercalation, and groove binding, depending on the substituents on the terpy ligand [31–35].

In this work, we present the systematic investigation of the potential of 7 Ru(II) complexes of the type $[Ru(terpy)(terpy\text{-}X)]^{2+}$ (X = H (**1**), Cl (**2**), Br (**3**), OMe (**4**), COOH (**5**), COOMe (**6**), NMe_2 (**7**)) as potential chemotherapeutic agents and as PDT PSs. All investigated complexes were fully characterized by ^{1}H and ^{13}C NMR, ESI-HRMS, elemental analysis as well as single crystal X-ray crystallography. As described below, one of the complexes (compound **7**) was found to be cytotoxic in the micromolar range in the dark as well as to have some phototoxicity upon light exposure at 480 nm, highlighting some potential for this type of complexes.

2. Experimental section

2.1. Materials

All chemicals were obtained from commercial sources and used without further purification. Solvents were dried over molecular sieves if necessary. The Ru(II) precursor $Ru(terpy)Cl_3$ was synthesised as previously published [36]. The substituted 2,2′:6′,2″-terpyridine ligands (terpy-X): 4′-chloro-2,2′:6′,2″-terpyridine (terpy-Cl) [37], 4′-bromo-2,2′:6′,2″-terpyridine (terpy-Br) [38], 4′-methoxy-2,2′:6′,2″-terpyridine (terpy-OMe) [39], 4′-carboxy-2,2′:6′,2″-terpyridine (terpy-COOH) [40], 4′-methylcarboxy-2,2′:6′,2″-terpyridine (terpy-COOMe) [40], 4′-dimethylamino-2,2′:6′,2″-terpyridine (terpy-NMe_2) [41] were synthesised as previously reported.

2.2. Instrumentation and methods

^{1}H and ^{13}C NMR spectra were recorded on a Bruker 400 MHz NMR spectrometer. Chemical shifts (δ) are reported in parts per million (ppm) referenced to tetramethylsilane (δ 0.00) ppm using the residual proton solvent peaks as internal standards. Coupling constants (J) are reported in Hertz (Hz) and the multiplicity is abbreviated as follows: s (singulet), d (doublet), dd (doublet of doublet), m (multiplet). ESI-MS experiments were carried out using a LTQ-Orbitrap XL from Thermo Scientific (Thermo Fisher Scientific, Courtaboeuf, France) and operated in positive ionization mode, with a spray voltage at 3.6 kV. No Sheath and auxiliary gas was used. Applied voltages were 40 and 100 V for the ion transfer capillary and the tube lens, respectively. The ion transfer capillary was held at 275 °C. Detection was achieved in the Orbitrap with a resolution set to 100,000 (at m/z 400) and a m/z range between 150 and 2000 in profile mode. Spectrum was analysed using the acquisition software XCalibur 2.1 (Thermo Fisher Scientific, Courtaboeuf, France). The automatic gain control (AGC) allowed accumulation of up to $2 * 10^5$ ions for FTMS scans, maximum injection time was set to 300 ms and 1 μscan was acquired. 10 μL was injected using a Thermo Finnigan Surveyor HPLC system (Thermo Fisher Scientific, Courtaboeuf, France) with a continuous infusion of methanol at 100 μL·min^{-1}. Elemental microanalyses were performed on a Thermo Flash 2000 elemental analyser.

2.3. Synthesis

$$[Ru(terpy)_2](PF_6)_2 \quad (1)$$

$[Ru(terpy)_2](PF6)_2$ was synthesised as previously published [42]. Experimental data fits with the literature. Purity of the sample was assessed by HPLC and elemental analysis. *Anal.* Calc. for $C_{30}H_{22}F_{12}N_6P_2Ru$: C 42.02, H 2.59, N 9.80. Found: C 41.91, H 2.60, N 9.71.

$$[Ru(terpy)(terpy{-}Cl)](PF_6)_2 \quad (2)$$

The synthesis of $[Ru(terpy)(terpy\text{-}Cl)](PF_6)_2$ was previously reported [43]. In this work, another synthetic route was employed. $Ru(terpy)Cl_3$ (200 mg, 0.45 mmol, 1.0 equiv.), 4′-Chloro-2,2′:6′,2″-terpyridine (terpy-Cl) (134 mg, 0.50 mmol, 1.1 equiv) and some drops of *N*-ethylmorpholine were dissolved in 8:2 EtOH/H_2O (50 mL). The mixture was heated under reflux for 4 h under nitrogen atmosphere. The crude product was cooled to room temperature and undissolved solid was filtered off over Celite. The solid was washed with EtOH, the solution concentrated and a sat. aqueous solution of NH_4PF_6 was added. The crude product, which precipitated as a PF_6 salt was collected by centrifugation and washed with EtOH, H_2O and Et_2O. The product was isolated by column chromatography on silica gel with an CH_3CN/aq. KNO_3 (0.4 M) solution (10:1). The fractions containing the product were united and the solvent was removed under reduced pressure. The residue was dissolved in CH_3CN and undissolved KNO_3 was removed by filtration. The solvent was removed again and the product was dissolved in H_2O (50 mL). Upon addition of NH_4PF_6 the product precipitated as a PF_6 salt. The solid was obtained by filtration and was washed three-times with H_2O and Et_2O. Experimental data fits with the literature. Purity of the sample was assessed by HPLC and elemental analysis. ESI-HRMS m/z: 301.0277 $[M]^{2+}$, calcd for $C_{30}H_{21}ClN_6Ru$ 301.0274. *Anal.* Calc. for $C_{30}H_{21}ClF_{12}N_6P_2Ru + 1.3 * H_2O$: C 39.36, H 2.60, N 9.18. Found: C 38.99, H 2.50, N 9.68.

$$[Ru(terpy)(terpy{-}Br)](PF_6)_2 \quad (3)$$

The synthesis of $[Ru(terpy)(terpy\text{-}Br)](PF_6)_2$ was previously reported [44]. In this work, another synthetic route was employed. $Ru(terpy)Cl_3$ (200 mg, 0.45 mmol, 1.0 equiv.), 4′-Bromo-2,2′:6′,2″-terpyridine (terpy-Br) (156 mg, 0.50 mmol, 1.1 equiv) and some drops of *N*-ethylmorpholine were dissolved in 8:2 EtOH/H_2O (50 mL). The mixture was heated under reflux for 4 h under nitrogen atmosphere. The crude product was cooled to room temperature and undissolved solid was filtered off over Celite. The solid was washed with EtOH, the solution concentrated and a sat. aqueous solution of NH_4PF_6 was added. The crude product, which precipitated as a PF_6 salt was collected by centrifugation and washed with EtOH, H_2O and Et_2O. The product was isolated by column chromatography on silica gel with an CH_3CN/aq. KNO_3 (0.4 M) solution (10:1). The fractions containing the product were united and the solvent was removed under reduced pressure. The residue was dissolved in CH_3CN and undissolved KNO_3 was removed by filtration. The solvent was removed again and the product was dissolved in H_2O (50 mL). Upon addition of NH_4PF_6 the product precipitated as a PF_6 salt. The solid was obtained by filtration and was washed three-times with H_2O and Et_2O. Experimental data fits with the literature. Purity of the sample was assessed by HPLC and elemental analysis. ESI-HRMS m/z: 324.0020 $[M]^{2+}$, calcd for $C_{30}H_{21}BrN_6Ru$ 324.0012. *Anal.* Calc. for $C_{30}H_{21}BrF_{12}N_6P_2Ru + 1\ H_2O$: C 37.75, H 2.43, N 8.81. Found: C 37.55, H 2.03, N 9.26.

$[Ru(terpy)(terpy{-}OMe)](PF_6)_2$ (4)

$Ru(terpy)Cl_3$ (203 mg, 0.46 mmol, 1.0 equiv.), 4′-Methoxy-2,2′:6′,2″-terpyridine (terpy-Br) (133 mg, 0.51 mmol, 1.1 equiv) and some drops of *N*-ethylmorpholine were dissolved in 8:2 EtOH/H_2O (50 mL). The mixture was heated under reflux for 5 h under nitrogen atmosphere. The crude product was cooled to room temperature and undissolved solid was filtered off over Celite. The solid was washed thoroughly with EtOH and afterwards the solvent was removed under reduced pressure. The residue was dissolved in H_2O and a sat. aqueous solution of NH_4PF_6 was added. The crude product, which precipitated as a PF_6 salt was collected by centrifugation and washed with EtOH, H_2O and Et_2O. The product was isolated by column chromatography on silica gel with an CH_3CN/aq. KNO_3 (0.4 M) solution (10:1). The fractions containing the product were united and the solvent was removed under reduced pressure. The residue was dissolved in CH_3CN and undissolved KNO_3 was removed by filtration. The solvent was removed again and the product was dissolved in H_2O (50 mL). Upon addition of NH_4PF_6 the product precipitated as a PF_6 salt. The solid was obtained by filtration and was washed three-times with H_2O and Et_2O. 257 mg of $[Ru(terpy)(terpy\text{-}OMe)](PF_6)_2$ (**4**) (0.29 mmol, 63%) were yielded as a red solid. ^{1}H NMR (CD_3CN, 400 MHz): δ = 8.72 (d, J = 8.2 Hz, 2H), 8.50–8.46 (m, 4H), 8.36 (t, J = 8.2 Hz, 1H), 8.33 (s, 2H), 7.93–7.86 (m, 4H), 7.42 (ddd, J = 5.5, 1.4, 0.7 Hz, 2H), 7.29 (ddd, J = 5.5, 1.4, 0.7 Hz, 2H), 7.18 (ddd, J = 7.5, 5.6 1.3 Hz, 2H), 7.12 (ddd, J = 7.5, 5.6 1.3 Hz, 2H), 4.31 (s, 3H). ^{13}C NMR (CD_3CN, 100 MHz): δ = 167.6, 158.8, 158.6, 156.5, 156.4, 153.3, 152.8, 138.5, 138.4, 135.7, 128.0, 127.9, 125.0, 124.8, 124.1, 111.3, 57.8. ESI-HRMS *m/z*: 299.0527 $[M]^{2+}$, calcd for $C_{31}H_{24}N_6O_1Ru$ 299.0522. *Anal.* Calc. for $C_{31}H_{24}F_{12}N_6O_2P_2Ru$: C 41.95, H 2.73, N 9.47. Found: C 41.79, H 2.64, N 9.45.

$[Ru(terpy)(terpy-COOH)](PF_6)_2$ (5)

The synthesis of $[Ru(terpy)(terpy\text{-}COOH)](PF_6)_2$ was previously reported [45]. In this work, another synthetic route was employed. $Ru(terpy)Cl_3$ (200 mg, 0.45 mmol, 1.0 equiv.), 4′-Carboxy-2,2′:6′,2″-terpyridine (terpy-COOH) (139 mg, 0.50 mmol, 1.1 equiv) and some drops of *N*-ethylmorpholine were dissolved in 8:2 EtOH/H_2O (50 mL). The mixture was heated under nitrogen atmosphere at reflux for 4 h. After cooling down to room temperature, the crude product was filtered over Celite and washed thoroughly with EtOH. The solvent was removed and the solid residue dissolved in H_2O. A sat. aqueous solution of NH_4PF_6 was added and the crude product precipitated as a PF_6 salt. The solid was collected by centrifugation and washed with Ethanol, Water and Et_2O. The product was isolated via fractionated precipitation from Acetonitrile by adding dropwise Et_2O. The yielded solid was isolated by filtration and washed with pentane. Experimental data fits with the literature. Purity of the sample was assessed by HPLC and elemental analysis. *Anal.* Calc. for $C_{31}H_{22}F_{12}N_6O_2P_2Ru + 0.1 * C_5H_{12}$: C 41.63, H 2.57, N 9.25. Found: C 41.84, H 2.68, N 9.56.

$[Ru(terpy)(terpy-COOMe)](PF_6)_2$ (6)

$Ru(terpy)Cl_3$ (137 mg, 0.31 mmol, 1.0 equiv.) and $AgBF_4$ (212 mg, 1.09 mmol, 3.5 equiv.) were suspended in Acetone (50 mL) under nitrogen atmosphere. The mixture was refluxed for 2 h, cooled to room temperature and undissolved solid was filtered off over Celite. The solid was washed with methanol and then the solvent removed under reduced pressure. The residue was dissolved in dry EtOH (50 mL) and 4′-Methylcarboxy-2,2′:6′,2″-terpyridine (terpy-COOMe) (100 mg, 0.34 mmol, 1.1 equiv.) was added. The mixture was heated under reflux for 18 h under nitrogen atmosphere. The crude product was cooled to room temperature and undissolved solid was filtered off over Celite. The solid was washed with EtOH, the solution concentrated and a sat. aqueous solution of NH_4PF_6 was added. The crude product, which precipitated as a PF_6 salt was collected by centrifugation and washed with EtOH, H_2O and Et_2O. The product was isolated by column chromatography on silica gel with an CH_3CN/aq. KNO_3 (0.4 M) solution (10:1). The fractions containing the product were united and the solvent was removed under reduced pressure. The residue was dissolved in CH_3CN and undissolved KNO_3 was removed by filtration. The solvent was removed again and the product was dissolved in H_2O (50 mL). Upon addition of NH_4PF_6 the product precipitated as a PF_6 salt. The solid was obtained by filtration and was washed three-times with H_2O and Et_2O. 154 mg of $[Ru(terpy)(terpy\text{-}COOMe)](PF_6)_2$ (**6**) (0.17 mmol, 55%) were yielded as a red solid. ^{1}H NMR (CD_3CN, 400 MHz): δ = 9.20 (s, 2H), 8.76 (d, J = 8.2 Hz, 2H), 8.66–8.62 (m, 2H), 8.50–8.47 (m, 2H), 8.45 (t, J = 8.2 Hz, 1H), 7.98–7.89 (m, 4H), 7.39–7.36 (m, 2H), 7.30–7.27 (m, 2H), 7.23–7.19 (m, 2H), 7.16–7.10 (m, 2H), 4.18 (s, 3H). ^{13}C NMR (CD_3CN, 100 MHz): δ = 165.4, 158.7, 158.4, 157.1, 155.8, 153.5, 153.4, 139.3, 139.1, 137.5, 137.2, 128.8, 128.4, 125.8, 125.5, 124.8, 123.7, 54.2. ESI-HRMS *m/z*: 313.0502 $[M]^{2+}$, calcd. for $C_{32}H_{24}N_6O_2Ru$ 313.0497. *Anal.* Calc. for $C_{32}H_{24}F_{12}N_6O_2P_2Ru$: C 41.98, H 2.64, N 9.18. Found: C 41.92, H 2.63, N 9.50.

$[Ru(terpy)(terpy{-}NMe_2)](PF_6)_2$ (7)

$Ru(terpy)Cl_3$ (205 mg, 0.47 mmol, 1.0 equiv.), 4′-Dimethylamino-2,2′:6′,2″-terpyridine (terpy- NMe_2) (141 mg, 0.52 mmol, 1.1 equiv) and some drops of *N*-ethylmorpholine were dissolved in 8:2 EtOH/H_2O (50 mL). The mixture was heated under reflux for 6 h under nitrogen atmosphere. The crude product was cooled to room temperature and undissolved solid was filtered off over Celite. The solid was washed thoroughly with EtOH and afterwards the solvent was removed under reduced pressure. The residue was dissolved in H_2O and a sat. aqueous solution of NH_4PF_6 was added. The crude product, which precipitated as a PF_6 salt was collected by centrifugation and washed with EtOH, H_2O and Et_2O. The product was isolated by column chromatography on silica gel with an CH_3CN/aq. KNO_3 (0.4 M) solution (10:1). The fractions containing the product were united and the solvent was removed under reduced pressure. The residue was dissolved in CH_3CN and undissolved KNO_3 was removed by filtration. The solvent was removed again and the product was dissolved in H_2O (50 mL). Upon addition of NH_4PF_6 the product precipitated as a PF_6 salt. The solid was obtained by filtration and was washed three-times with H_2O and Et_2O. The product was isolated via fractionated precipitation from CH_3CN by adding dropwise Et_2O. 225 mg of $[Ru(terpy)(terpy\text{-}NMe_2)](PF_6)_2$ (**7**) (0.25 mmol, 53%) were yielded as a dark red solid. ^{1}H NMR (CD_3CN, 400 MHz): δ = 8.70 (d, J = 8.2 Hz, 2H), 8.52–8.45 (m, 4H), 8.31 (t, J = 8.2 Hz, 1H), 7.93 (s, 2H), 7.93–7.82 (m, 4H), 7.50–7.48 (m, 2H), 7.24–7.19 (m, 4H), 7.08–7.03 (m, 2H), 3.46 (s, 6H). ^{13}C NMR (CD_3CN, 100 MHz): δ = 159.9, 159.4, 157.3, 156.3, 154.8, 153.5, 152.9, 138.6, 138.5, 135.2, 128.3, 127.7, 125.0, 124.7, 124.3, 107.4, 40.8. ESI-HRMS *m/z*: 305.5687 $[M]^{2+}$, calcd. for $C_{32}H_{27}N_7Ru$ 305.5680. *Anal.* Calc. for $C_{32}H_{27}F_{12}N_7P_2Ru$: C 42.68, H 3.02, N 10.89. Found: C 42.55, H 2.95, N 10.82.

2.4. X-ray crystallography

X-ray single-crystal data were collected at 160(1) K with Oxford liquid-nitrogen Cryostream coolers on Rigaku OD diffractometers: SuperNova (CCD Atlas detector) for **1_BPh$_4$** and XtaLAB Synergy Dualflex (Pilatus 200 K detector) for all the other X-ray analyses. Single wavelength X-ray sources from micro-focus sealed X-ray tubes were used with the Mo K_α radiation (λ = 0.71073 Å) [46] for **1_BPh$_4$** and **2_BPh$_4$** and with the Cu K_α radiation (λ = 1.54184 Å) [46] for all other analyses. The selected single crystals were mounted using polybutene oil on a flexible loop fixed on a goniometer head and transferred to the diffractometer. Pre-experiments, data collections, data reductions and analytical absorption corrections [47] were performed with the program suite *CrysAlisPro* [48]. Using *Olex2* [49], all structures were solved with the SHELXT [50] small molecule structure solution program and refined with the *SHELXL2018/3* program package [51] by full-matrix least-squares minimization on F^2. Molecular graphics were

generated using *Mercury 4.0* [52]. The crystal data collections and structure refinement parameters for are summarized in Tables S1–S9. CCDC 1889454 (for **2_PF$_6$**), 1889455 (for **2_BF$_4$**), 1889456 (for **3_BF$_4$**), 1889457 (for **3_PF$_6$**), 1889458 (for **4_BF$_4$**), 1889459 (for **2_BPh$_4$**), 1889460 (for **4_PF$_6$**), 1889461 (for **6_BPh$_4$**), 1889462 (for **6_PF$_6$**), 1889463 (for **6_BF$_4$**), 1889464 (for **5_BPh$_4$**), 1889465 (for **7_PF$_6$**), 1889466 (for **terpy-Br**), 1889467 (for **7_BF$_4$**), 1889468 (for **5_BF$_4$**), 1889469 (for **terpy-Cl**) and 1889470 (for **1_BPh$_4$**) contain the supplementary crystallographic data for these compounds, and can be obtained free of charge from the Cambridge Crystallographic Data Centre via www.ccdc.cam.ac.uk/data_request/cif.

2.5. Spectroscopic measurements

The absorption of the samples has been measured with a SpectraMax M2 Spectrometer (Molecular Devices). The emission was measured by irradiation of the sample in fluorescence quartz cuvettes (width 1 cm) using a NT342B Nd-YAG pumped optical parametric oscillator (Ekspla) at 450 nm. Luminescence was focused and collected at right angle to the excitation pathway and directed to a Princeton Instruments Acton SP-2300i monochromator. As a detector a PI-Max 4 CCD camera (Princeton Instruments) has been used.

2.6. Luminescence quantum yield measurements

For the determination of the luminescence quantum yield, the samples were prepared in a non-degassed CH_3CN solution with an absorbance of 0.1 at 450 nm. This solution was irradiated in fluorescence quartz cuvettes (width 1 cm) using a NT342B Nd-YAG pumped optical parametric oscillator (Ekspla) at 450 nm. The emission signal was focused and collected at right angle to the excitation pathway and directed to a Princeton Instruments Acton SP-2300i monochromator. As a detector a PI-Max 4 CCD camera (Princeton Instruments) has been used. The luminescence quantum yields were determined by comparison with the reference $[Ru(bipy)_3]Cl_2$ in CH_3CN (Φ_{em} = 0.059) [53] applying the following formula:

$$\Phi_{em,sample} = \Phi_{em,reference} * (F_{reference}/F_{sample}) * (I_{sample}/I_{reference}) * (n_{sample}/n_{reference})^2$$

$$F = 1–10^{-A}$$

Φ_{em} = luminescence quantum yield, F = fraction of light absorbed, I = integrated emission intensities, n = refractive index, A = absorbance of the sample at irradiation wavelength.

2.7. Lifetime measurements

For the determination of the lifetimes, the samples were prepared in an air saturated and in a degassed CH_3CN solution with an absorbance of 0.1 at 450 nm. This solution was irradiated in fluorescence quartz cuvettes (width 1 cm) using a NT342B Nd-YAG pumped optical parametric oscillator (Ekspla) at 450 nm. The emission signal was focused and collected at right angle to the excitation pathway and directed to a Princeton Instruments Acton SP-2300i monochromator. As a detector a R928 photomultiplier tube (Hamamatsu) has been used.

2.8. Distribution coefficient

The lipophilicity of a compound was determined by measuring its distribution coefficient between the PBS and octanol phase by using the “shake-flask” method. For this technique, the used phases were previously saturated in each other. The compound was dissolved in the phase (A) with its major presence with an absorbance of about 0.5 at 450 nm. This solution was then mixed with an equal volume of the other phase (B) at 80 rpm for 8 h with an Invitrogen sample mixer and equilibrated overnight. The phase A was then carefully separated from phase B. The amount of the compound before and after the sample mixing was determined by UV/VIS spectroscopy at 450 nm with a SpectraMax M2 Microplate Reader (Molecular Devices). The evaluation of the complexes was repeated three times and the ratio between the organic and aqueous phase calculated.

2.9. Stability in human plasma

The stability of the complexes was evaluated with caffeine as an internal standard, which has already shown to be suitable for these experiments [54]. The pooled human plasma was obtained from Biowest and caffeine from TCI Chemicals. Stock solutions of the compounds and caffeine were prepared in DMSO. One aliquot of the solutions was added to 975 µL of human plasma to a total volume of 1000 µL. Final concentrations of the compounds of 50 µM and caffeine of 25 µM were achieved. The resulting solution was incubated for 48 h at 37 °C with continuous gentle shaking (ca. 300 rpm). The reaction was stopped after the incubation time by addition of 4 mL of methanol. The mixture was centrifuged for 45 min at 6504*g* at 4 °C. The methanolic solution was filtered through a 0.2 µm membrane filter. The solvent was evaporated under reduced pressure and the residue was dissolved in 1:1 (v/v) CH_3CN/H_2O 0.1% TFA solution. The solution was filtered through a 0.2 µm membrane filter and analysed using a 1260 Infinity HPLC System (Agilent Technology). A Pursuit XRs 5 C18 (250 × 4.6 mm) reverse phase column has been used and the absorption at 250 nm measured. The samples have been measured with a flow rate of 1 mL/min and a linear gradient of 0.1% TFA containing H_2O and CH_3CN (t = 0–3 min 95% H_2O 0.1% TFA, 5% CH_3CN; t = 17 min 100% CH_3CN; t = 23 min 100% CH_3CN) has been used.

2.10. Photostability

The samples were prepared in an air saturated CH_3CN solution. To measure the photostability, the samples were irradiated at 450 nm (light dose after 10 min: 13.22 J/cm^2) in 96 well plates with an Atlas Photonics LUMOS BIO irradiator during time intervals from 0 to 10 min. The absorbance spectrum from 350 to 700 nm was recorded with a SpectraMax M2 Microplate Reader (Molecular Devices) after each time interval and compared. As a positive control $[Ru(bipy)_3]Cl_2$ and as a negative control Protoporphyrin IX has been used.

2.11. Cell culture

HeLa cells were cultured in DMEM medium supplemented with 10% fetal calf serum. RPE-1 cells were cultured in DMEM/F-12 medium supplemented with 10% fetal calf serum. Cell lines were complemented with 100 U/mL penicillin-streptomycin mixture, and maintained in humidified atmosphere at 37 °C and 5% of CO_2. Before an experiment, cells were passaged three times.

2.12. (Photo-)cytotoxicity

The cytotoxicity of the compounds was accessed by measuring the cell viability using a fluorometric resazurin assay. Cells were seeded in triplicates in 96 well plates (4000 cells per well in 100 µL of media). After 24 h, media was removed and the cells were treated with increasing concentrations of the compounds diluted in cell media achieving a total volume of 200 µL. The cells were incubated with the compounds for 4 h. After this time, the media was removed and replaced with 200 µL of fresh media. For the phototoxicity studies, the cells were exposed to light with an Atlas Photonics LUMOS BIO irradiator. Each well was constantly illuminated with 480 nm irradiation. During this time, the temperature was maintained at 37 °C. The cells were grown in the incubator for additional 44 h. For the determination of the dark cytotoxicity, the cells were not irradiated and after the

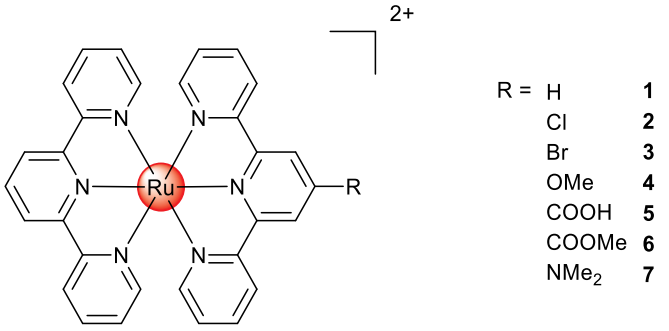

Fig. 1. Chemical structures of the $[Ru(terpy)(terpy\text{-}X)]^{2+}$ complexes investigated in this work. The complexes were isolated as PF_6 salts.

media exchange directly incubated for 44 h. After this time, media was replaced with fresh media containing resazurin with a final concentration of 0.2 mg/mL. After 4 h incubation, the amount of the fluorescent product resorufin was determined upon excitation at 540 nm and measurement its emission at 590 nm using a SpectraMax M2 Microplate Reader (Molecular Devices). The obtained data was analysed with the GraphPad Prism software.

3. Results and discussion

3.1. Syntheses and characterisation

Ru(II) complexes **1–7** investigated in this work can be visualised in Fig. 1. The synthesis and characterisation of compounds **1** [42], **2** [43], **3** [44] and **5** [45] have been previously reported in the literature. However, in this work, except for **1**, a different synthetic procedure was employed to prepare them. To the best of our knowledge, complexes **4**, **6** and **7** have never been reported. Specifically, the substituted 2,2′:6′,2″-terpyridine ligands (terpy-X, Scheme S1), namely 4′-chloro-2,2′:6′,2″-terpyridine (terpy-Cl) [37], 4′-bromo-2,2′:6′,2″-terpyridine (terpy-Br) [38], 4′-methoxy-2,2′:6′,2″-terpyridine (terpy-OMe) [39], 4′-carboxy-2,2′:6′,2″-terpyridine (terpy-COOH) [40], 4′-methylcarboxy-2,2′:6′,2″-terpyridine (terpy-COOMe) [40] and 4′-dimethylamino-2,2′:6′,2″-terpyridine (terpy-NMe_2) [41] were synthesised as previously reported. Analytical data of all synthesised ligands matched with those of the literature. Interestingly, the structures of the ligands terpy-Cl and terpy-Br were confirmed by single crystal X-ray crystallography in this work (see section below). Complexes were synthesised by refluxing the precursor $Ru(terpy)Cl_3$ [36] and the respective terpy ligand in ethanol to give complexes **1–7** (Scheme S2) in moderate yields [36]. Worthy of note, the reaction between $Ru(terpy)Cl_3$ with terpy-COOMe yielded a mixture of different undesired products, as observed by HPLC (data not shown). To overcome this problem, the synthetic procedure was changed to a two-step reaction. In the first step, the Cl substituents on the Ru(II) core were exchanged with solvent molecules by reaction of $Ru(terpy)Cl_3$ with $AgBF_4$ and filtration of the formed AgCl. In the second step, the terpy-COOMe ligand was coordinated to the metal core upon replacement of the solvent molecules. All complexes were analysed by ^1H, ^{13}C NMR, ESI-HRMS as well elemental analysis (Figs. S1–S9). Worthy of note, the structures of all Ru(II) complexes prepared in this work were determined by single crystal X-ray crystallography (see below).

3.2. X-ray crystallography

The crystal structures of terpy-Cl, terpy-Br, and all investigated $[Ru(terpy)(terpy\text{-}X)]^{2+}$ complexes **1–7** have been determined by single crystal X-ray diffraction studies. Crystal data, structure refinement parameters and molecular structures are presented in Tables S1–S9 and Figs. S10–S18. In the literature, the $[Ru(terpy)_2]^{2+}$ cation is well known and can be found in many crystal structures co-crystallizing with various counterions (Cl^-, I, BF_4^-, ClO_4^-, PF_6^- and other Pt anionic clusters…) and solvent molecules (H_2O, CH_2Cl_2, MeCN, NMe_2CHO…) [42,55–63]. There is also a very large number of other ruthenium terpyridine complexes in the Cambridge Structural Database (version 5.40, last update November 2018) [64]. For instance, 142 structures were obtained from a search with terpyridine ligands substituted in *para* position. In the crystal structures of our new metal complexes, the Ru(II) centres are typically in a distorted octahedral environment coordinated by two terpyridine ligands acting as tridentate pincer ligands through the nitrogen atoms. The two ligand planes are always exactly or almost perpendicular to each other. The largest deviation to orthogonality is observed in **6_PF$_6$** with an angle of 86.9(3)° between the calculated mean planes. As a structural feature, the M–$N_{central}$ distances are significantly shorter than the M–$N_{terminal}$ distances which is typical for coordination of conjugated terimine systems. The M–$N_{central}$ distances fall in the range 1.973(3) – 1.998(3) Å and the M–$N_{terminal}$ distances in the range 2.063(2) – 2.089(9) Å. In most of the crystal structures of **2–7**, the Ru(II) molecules exhibit a positional disorder of the terpyridine ligands. The result of such a disorder is that the group or atom in *para* position on the central pyridine of the substituted terpyridine ligand (and consequently the corresponding H atom of the unsubstituted ligand as well) appears on both terpyridine ligands with a site-occupancy factor of 0.5. It is observed in nine crystal structures over fourteen, only **4_PF$_6$**, **5_BF$_4$**, **6_PF$_6$**, **7_PF$_6$** and **7_BF$_4$** are free of that kind of disorder. It seems to not be influenced or controlled by the presence of one specific counter ion, neither by the *para* substituent but it is worth noting that when the latter is a “mono-atomic” group like in complexes **2** and **3** (X = Cl, Br) the disorder is always observed (five crystal structures). The crystal packing of $[M(terpy)_2]$ cations have been fully analysed by Scudder et al. in 1999 [65]. A standard crystal supramolecular motif has been identified as a two-dimensional net of terpy embraces involving molecules attracted by face-to-face π…π interactions and edge-to-face C-H…π interactions between the external rings of the ligands. Despite the para substitution of one of the terpyridine ligands, this standard “terpy embrace” motif can be observed in six of our crystal structures: **2_BF$_4$**, **2_PF$_6$**, **3_BF$_4$**, **3_PF$_6$**, **4_BF$_4$** and **7_BF$_4$** (Fig. S19). The presence of the bulky BPh_4^- couterion in **1_BPh$_4$**, **2_BPh$_4$**, **5_BPh$_4$** and **6_BPh$_4$** rules out that standard layer structure since no direct interactions are observed between cations anymore, the crystal packing is mainly governed by π…π interactions between the pyridine rings of the cations and the phenyl rings of the anions (Fig. S20). The so-called terpy embrace motif still exists in the other crystal structures but the typical face-to-face and edge-to-face interactions only lead to chains in **5_BF$_4$** and **7_PF$_6$** (Fig. S21) or form small units of two molecules in **6_PF$_6$** or four molecules in **6_BF$_4$** (Fig. S22). These chains or units are further connected to via C-H…O hydrogen bondings or C-H…π interactions, and to the counterions via C-H…F interactions to form a three-dimensional network. Finally, the crystal structure of **4_PF$_6$** is the only one to not exhibit π…π interactions, only C-H…π and C-H…F interactions are observed.

3.3. Photophysical characterisation

For a complete characterisation, the absorption and emission properties of the synthesised compounds were investigated. The UV/Vis absorption spectra were recorded in CH_3CN (Fig. 2) and PBS buffer (Fig. S23). The comparison between the different complexes shows that the *para* substituents on the central pyridine of the terpy ligand influence the amount of light absorbed and therefore the excitation coefficient (Table S10). However, no strong shift either to blue or red could be observed. The analysis of the absorption shows that the very intensive band in the UV region is caused by a ligand centred (LC) π-π* transition. The other broad band in the visible spectrum (~400–550 nm) was attributed to the spin-allowed d-π metal-to-ligand charge transfer (MLCT) transition [20,25,66]. Next to the absorption, the emission of

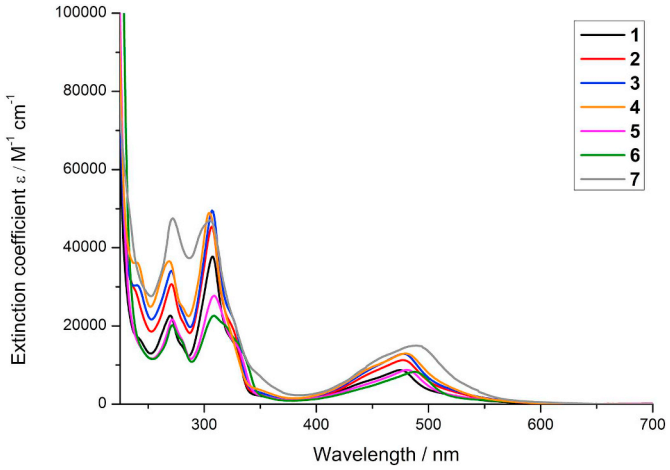

Fig. 2. UV/Vis spectra of the complexes **1–7** in CH_3CN.

the complexes was investigated. The synthesised complexes have a very weak emission from ~550–800 nm (Table S1, Fig. S24) upon excitation in CH_3CN at 450 nm at room temperature which was measurable only at the detection limit of our used setup. The luminescence quantum yields were found to be < 0.01% in CH_3CN which is fitting with previous studies of similar complexes [30,67–69]. For verification that the measured emission is caused by the compounds, the excitation and absorption spectrum of compound **6** has been compared. As expected, no significant differences between the spectra could be observed. The characterisation of the excited state lifetimes was not possible with our apparatus due to a necessary minimal delay between excitation and detection, indicating that the compounds **1–7** have lifetimes < 29 ns. Therefore, as expected, the excited state lifetimes are in the same range than other $[Ru(terpy)_2]^{2+}$ derivatives previously published [30,67–69].

3.4. Determination of the logP values

After having assessed the photophysical properties of our compounds, we investigated their solubility in an aqueous solution which is crucial for any kind of biological application. For this purpose, we determined the distribution coefficient (log*P* values) of the complexes between an aqueous PBS phase and a lipophilic octanol phase by the "shake-flask" method, as previously performed by our group with other metal complexes [70,71]. All compounds were mostly found in the aqueous phase, which we assume, is due to the positive charge of the metal complexes. As anticipated, the results (Fig. 3) show that the log*P* values change based on the functional group present on the terpy ligand. Compound **5** bearing a carboxylic acid was found to be the most hydrophilic and complex **3** bearing a bromine substituent the most lipophilic one. The following order could be made (from the most hydrophilic to the most lipophilic): **5** > **1** > **6** > **2** > **4** > **7** > **3**.

3.5. Stability in human plasma

In order to have a preliminary insight of the metabolic stability of our compounds, their compatibility under biological conditions was investigated. For this purpose, the complexes were incubated upon the addition of the internal standard caffeine in human plasma at 37 °C for 48 h and their stability investigated, as previously performed by our group with other metal complexes [21,23]. After extraction from the plasma, the complexes were analysed via HPLC and the chromatogram before and after incubation compared. Complexes **1–5** and **7** (Figs. S25–S29, S31) were found to be stable for a therapeutically relevant time. However, some degradation of compound **6** (Fig. S30) was observed, as indicated by the appearance of small peaks as well as a decreased of the compound/caffeine ratio.

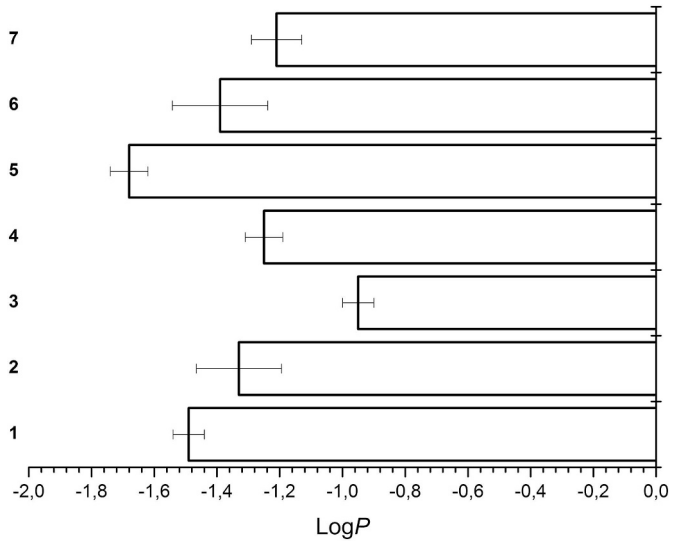

Fig. 3. Distribution coefficients (Log*P* values) of complexes **1–7**.

3.6. Photostability

Since Ru(II) complexes are well known to act as PDT PSs, the compounds were investigated to assess if a phototobleaching effect, which is a degradation of the compound upon light irradiation, was observed [72,73]. To investigate this, the complexes were constantly irradiated at 450 nm in CH_3CN and the potential change in absorbance between 350 and 700 nm from 0 to 10 min monitored. As a positive control, $[Ru(bipy)_3]Cl_2$ [74] (Fig. S32) and as a negative control Protoporphyrin IX (PpIX) [75] (Fig. S33) were chosen. Analyses (Figs. S34–S40) shows a different photostability of the complexes based on the functional group they bear. In general, a rather small photobleaching effect was observed. From comparison between the different complexes, the following order for photostability can be made from the most photostable to the least photostable: **2–3** > **4** > **1** > **7** > **5** > **6**.

3.7. Dark cytotoxicity and (photo-)toxicity

We then investigated the biological influence of the complexes **1–7**, their corresponding ligands and precursor on non-cancerous retinal pigment epithelium (RPE-1) and human cervical carcinoma (HeLa) cells. For this purpose, cells were treated with the compounds in the dark as well as upon light irradiation at 480 nm and their cell viability measured using a fluorometric resazurin assay. The IC_{50} values of the compounds are shown in Table 1. Unfortunately, complexes **1–6** did not show a measurable cytotoxic effect in HeLa cells in the dark as well as upon light irradiation. The poor phototoxic effect was expected due to the poor photophysical properties including the short excited state lifetimes of our complexes. However, compound **7** was found to be cytotoxic in the micromolar range in RPE-1 and HeLa cells. Unfortunately, no selectivity for cancerous cells versus non-cancerous cells was observed. The IC_{50} values for **7** are 1.4 times higher in RPE-1 and 3.3 times higher in HeLa cells than for the clinically used drug cisplatin. In terms of PDT treatment, an important value for the evaluation of a PS is the comparison between a dark and light treatment. For this purpose, the phototoxic index (PI) is defined as the ratio between the IC_{50} value in the dark and upon irradiation. Compound **7** was found to be phototoxic with a PI value of 1.4 in RPE-1 and HeLa cells. These values are rather low in comparison to porphyrin based-PSs like Protoporphyrin IX (PpIX). Additionally, the cytotoxic effects of the differently substituted terpy ligands were investigated (Table 1) in the dark as well as upon light exposure. Contrary to the cytotoxicity of the complexes, all the

Table 1
IC_{50} values in the dark and upon irradiation at 480 nm for the complexes **1–7**, the terpy-X ligands and the Ru-precursor incubated in non-cancerous retinal pigment epithelium (RPE-1) and human cervical carcinoma (HeLa) cells. Average of three independent measurements.

Compound	RPE-1			HeLa		
	IC_{50}/μM dark	IC_{50}/μM 480 nm (10 min, 3.1 J/cm^2)	PI	IC_{50}/μM dark	IC_{50}/μM 480 nm (10 min, 3.1 J/cm^2)	PI
1	> 100	> 100	n.d.	> 100	> 100	n.d.
2	> 100	> 100	n.d.	> 100	> 100	n.d.
3	> 100	> 100	n.d.	> 100	> 100	n.d.
4	> 100	> 100	n.d.	> 100	> 100	n.d.
5	> 100	> 100	n.d.	> 100	> 100	n.d.
6	> 100	> 100	n.d.	> 100	> 100	n.d.
7	39.7 ± 3.6	27.5 ± 1.1	1.4	35.1 ± 0.6	24.5 ± 2.6	1.4
terpy-H	21.8 ± 0.7	21.9 ± 2.4	1.0	26.5 ± 3.0	18.1 ± 0.7	1.5
terpy-Cl	8.7 ± 0.8	8.4 ± 1.2	1.0	12.3 ± 0.6	8.3 ± 1.3	1.5
terpy-Br	10.5 ± 0.4	8.8 ± 0.3	1.2	13.7 ± 3.2	6.9 ± 0.1	2.0
terpy-OMe	18.9 ± 0.8	16.7 ± 0.7	1.1	40.9 ± 2.1	40.2 ± 0.3	1.0
terpy-COOH	> 100	> 100	n.d.	50.5 ± 9.1	37.5 ± 5.4	1.3
terpy-COOMe	> 100	> 100	n.d.	23.3 ± 4.0	20.0 ± 2.4	1.2
terpy-NMe_2	14.8 ± 1.4	13.3 ± 2.2	1.1	19.6 ± 1.3	17.7 ± 2.7	1.1
Ru(Terpy)Cl_3	> 100	> 100	n.d	96.0 ± 3.5	87.5 ± 8.0	1.1
PpIX	> 100	3.8 ± 0.1	> 26	> 100	2.5 ± 0.1	> 40
Cisplatin	29.3 ± 1.4	–	–	10.5 ± 0.8	–	–

n.d. = not determinable.

ligands except of terpy-COOH and terpy-COOMe were toxic in the micromolar range. The exposure to light revealed phototoxicity with PI values in the range 1.0–2.0. Terpy ligands are well known to bind to biological relevant metals as for example Cu(II) inside of cells or living organisms and therefore their properties have been investigated as imaging probes and potential anticancer agents [76,77]. As the terpy ligands itself are not able to cause such a phototoxic effect, we assume that they could potentially bind with a biological relevant metal ion and the resulting complex could cause this effect.

4. Conclusion

In this study, we report on the systematic investigation of differently substituted $[Ru(terpy)(terpy\text{-}X)]^{2+}$ (X = H (**1**), Cl (**2**), Br (**3**), OMe (**4**), COOH (**5**), COOMe (**6**), NMe_2 (**7**)) complexes as potential chemotherapeutic agents and PDT PSs. The compounds were characterized in-depth including by single crystal X-ray crystallography. Photophysical measurements showed that the complexes strongly absorb in the green region of the visible electromagnetic spectrum. Further analysis revealed that they are weakly luminescent and have a short lived excited state. Despite their unfavourable photophysical properties such as a weak emission and short lifetimes, ruthenium terpyridine complexes were found in the past to be able to bind to DNA and to cleave it upon light irradiation. Inspired by the works of Thorp and Brewer et al. [26-30], we systematically evaluated their potential as PDT PSs. The distribution coefficient (log*P* value) of the complexes between an aqueous PBS phase and a lipophilic octanol phase was determined. As expected, all compounds were majorly found in the aqueous phase. Importantly, compounds **1–5** and **7** were found to be stable in human plasma and to have only a small photobleaching effect upon continuous LED irradiation. Complex **6** was found to be not stable in human plasma. Biological evaluation on one cancerous and one non-cancerous cell line demonstrated that compounds **1–6** had no cytotoxic effect in the dark as well as upon light irradiation. In comparison, **7** was found to have a dark and (photo-)cytotoxicity in the micromolar range. However, irradiation at 480 nm seems to have only a negligible effect. We assume that this is caused by the very short excited state lifetimes of this complex. Overall, this study demonstrates that small structural changes are able to influence significantly the effect that a compound has on cell viability.

Acknowledgements

This work was financially supported by an ERC Consolidator Grant PhotoMedMet to G.G. (GA 681679) and has received support under the program “Investissements d' Avenir” launched by the French Government and implemented by the ANR with the reference ANR-10-IDEX-0001-02 PSL (G.G.).

Appendix A. Supplementary data

Supplementary data to this article can be found online at https://doi.org/10.1016/j.jinorgbio.2019.110752.

References

[1] D. Cella, E. Cherin, Compr. Ther. 14 (1988) 69–75.
[2] A. Jemal, F. Bray, M.M. Center, J. Ferlay, E. Ward, D. Forman, CA Cancer J. Clin. 61 (2011) 69–90.
[3] A. Urruticoechea, R. Alemany, J. Balart, A. Villanueva, F. Vinals, G. Capella, Curr. Pharm. Des. 16 (2010) 3–10.
[4] E.R. Jamieson, S.J. Lippard, Chem. Rev. vol. 99, American Chemical Society, 1999, pp. 2467–2498.
[5] R. Oun, Y.E. Moussa, N.J. Wheate, Dalton Transactions, vol. 47, The Royal Society of Chemistry, 2018, pp. 6645–6653.
[6] L. Zeng, P. Gupta, Y. Chen, E. Wang, L. Ji, H. Chao, Z.-S. Chen, Chem. Soc. Rev. 46 (2017) 5771–5804.
[7] A. Notaro, G. Gasser, Chem. Soc. Rev. 46 (2017) 7317–7337.
[8] F. Li, J.G. Collins, F.R. Keene, Chem. Soc. Rev. 44 (2015) 2529–2542.
[9] F.R. Keene, J.A. Smith, J.G. Collins, Coord. Chem. Rev. 253 (2009) 2021–2035.
[10] S. Monro, K.L. Colón, H. Yin, J. Roque III, P. Konda, S. Gujar, R.P. Thummel, L. Lilge, C.G. Cameron, S.A. McFarland, Chem. Rev. 119 (2019) 797–828.
[11] C. Mari, V. Pierroz, S. Ferrari, G. Gasser, Chem. Sci. 6 (2015) 2660–2686.
[12] M. Jakubaszek, B. Goud, S. Ferrari, G. Gasser, Chem. Commun. 54 (2018) 13040–13059.
[13] F. Heinemann, J. Karges, G. Gasser, Acc. Chem. Res. 50 (2017) 2727–2736.
[14] K. Qiu, Y. Chen, T.W. Rees, L. Ji, H. Chao , Coord. Chem. Rev. 378 (2017) 66–86, https://doi.org/10.1016/j.ccr.2017.10.022.
[15] A. Yadav, T. Janaratne, A. Krishnan, S.S. Singhal, S. Yadav, A.S. Dayoub, D.L. Hawkins, S. Awasthi, F.M. MacDonnell, Mol. Cancer Ther. 12 (5) (**2013**) 643–653.
[16] F.E. Poynton, S.A. Bright, S. Blasco, D.C. Williams, J.M. Kelly, T. Gunnlaugsson, Chem. Soc. Rev. vol. 46, The Royal Society of Chemistry, 2017, pp. 7706–7756.
[17] J. Shum, P.K.-K. Leung, K.K.-W. Lo, Inorg. Chem, vol. 58, American Chemical Society, 2019, pp. 2231–2247.
[18] A. Juris, V. Balzani, F. Barigelletti, S. Campagna, P.l. Belser, A. Von Zelewsky, Coord. Chem. Rev. 84 (1988) 85–277.

[19] K. Kalyanasundaram, Coord. Chem. Rev. 46 (1982) 159–244.
[20] S. Campagna, F. Puntoriero, F. Nastasi, G. Bergamini, V. Balzani, V. Balzani, S. Campagna (Ed.), Photochemistry and Photophysics of Coordination Compounds I, Springer Berlin Heidelberg, Berlin, Heidelberg, 2007, pp. 117–214.
[21] C. Mari, V. Pierroz, R. Rubbiani, M. Patra, J. Hess, B. Spingler, L. Oehninger, J. Schur, I. Ott, L. Salassa, Chem. Eur. J. 20 (2014) 14421–14436.
[22] Y. Ellahioui, M. Patra, C. Mari, R. Kaabi, J. Karges, G. Gasser, S. Gómez-Ruiz, Dalton Trans. 48 (2019) 5940–5951.
[23] H. Huang, B. Yu, P. Zhang, J. Huang, Y. Chen, G. Gasser, L. Ji, H. Chao, Angew. Chem. Int. Ed. 54 (2015) 14049–14052.
[24] J. Karges, F. Heinemann, F. Maschietto, M. Patra, O. Blacque, I. Ciofini, B. Spingler, G. Gasser, A Ru(II) polypyridyl complex bearing aldehyde functions as a versatile synthetic precursor for long-wavelength absorbing photodynamic therapy photosensitizers, Bioorg. Med.Chem. 27 (12) (2015) 2666–2675, https://doi.org/10.1016/j.bmc.2019.05.011.
[25] J.P. Sauvage, J.P. Collin, J.C. Chambron, S. Guillerez, C. Coudret, V. Balzani, F. Barigelletti, L. De Cola, L. Flamigni, Chem. Rev. 94 (1994) 993–1019.
[26] N. Grover, N. Gupta, P. Singh, H.H. Thorp, Inorg. Chem. 31 (1992) 2014–2020.
[27] B.T. Farrer, H.H. Thorp, Inorg. Chem. 39 (2000) 44–49.
[28] N. Grover, H.H. Thorp, J. Am. Chem. Soc. 113 (1991) 7030–7031.
[29] G.A. Neyhart, N. Grover, S.R. Smith, W.A. Kalsbeck, T.A. Fairley, M. Cory, H.H. Thorp, J. Am. Chem. Soc. 115 (1993) 4423–4428.
[30] A. Jain, C. Slebodnick, B.S. Winkel, K.J. Brewer, J. Inorg. Biochem. 102 (2008) 1854–1861.
[31] K.K. Patel, E.A. Plummer, M. Darwish, A. Rodger, M.J. Hannon, J. Inorg. Biochem. 91 (2002) 220–229.
[32] C.-W. Jiang, H. Chao, H. Li, L.-N. Ji, J. Inorg. Biochem. 93 (2003) 247–255.
[33] Y. Liu, R. Hammitt, D.A. Lutterman, R.P. Thummel, C. Turro, Inorg. Chem. 46 (2007) 6011–6021.
[34] H.-Y. Ding, X.-S. Wang, L.-Q. Song, J.-R. Chen, J.-H. Yu, B.-W. Zhang, J. Photochem. Photobiol. A Chem. 177 (2006) 286–294.
[35] A. Rilak, I. Bratsos, E. Zangrando, J. Kljun, I. Turel, Z.i.D. Bugarčić, E. Alessio, Inorg. Chem. 53 (2014) 6113–6126.
[36] B.P. Sullivan, J.M. Calvert, T.J. Meyer, Inorg. Chem. 19 (1980) 1404–1407.
[37] E.C. Constable, M.D. Ward, J. Chem. Soc. Dalton Trans. (1990) 1405–1409.
[38] S. Katagiri, R. Sakamoto, H. Maeda, Y. Nishimori, T. Kurita, H. Nishihara, Chem Eur J 19 (2013) 5088–5096.
[39] E.C. Constable, K. Harris, C.E. Housecroft, M. Neuburger, J.A. Zampese, CrystEngComm 12 (2010) 2949–2961.
[40] M.W. Cooke, P. Tremblay, G.S. Hanan, Inorg. Chim. Acta 361 (2008) 2259–2269.
[41] E. Constable, A.C. Thompson, D. Tocher, M. Daniels, New J. Chem. 16 (1992) 855–867.
[42] S. Mallakpour, M. Dinari, H. Hadadzadeh, M. Daryanavard, F. Roudi, J. Fluoresc. 24 (2014) 1841–1848.
[43] E.C. Constable, P. Harverson, C.E. Housecroft, E. Nordlander, J. Olsson, Polyhedron 25 (2006) 437–458.
[44] E.C. Constable, R.W. Handel, C.E. Housecroft, A. Farràn Morales, B. Ventura, L. Flamigni, F. Barigelletti, Chem Eur J 11 (2005) 4024–4034.
[45] E.M. Hahn, N. Estrada-Ortiz, J. Han, V.F. Ferreira, T.G. Kapp, J.D. Correia, A. Casini, F.E. Kühn, Eur. J. Inorg. Chem. 2017 (2017) 1667–1672.
[46] Rigaku Oxford Diffraction, (2015).
[47] R. Clark, J. Reid, Acta Crystallogr. Sect. A: Found. Crystallogr. 51 (1995) 887–897.
[48] CrysAlisPro (version 1.171.38.41), Rigaku Oxford Diffraction, (2016).
[49] O.V. Dolomanov, L.J. Bourhis, R.J. Gildea, J.A.K. Howard, H. Puschmann, J. Appl. Crystallogr. 42 (2009) 339–341.
[50] G.M. Sheldrick, Acta Crystallographica Section A: Foundations and Advances 71 (2015) 3–8.
[51] G.M. Sheldrick, Acta Crystallographica Section C: Structural Chemistry 71 (2015) 3–8.
[52] C.F. Macrae, P.R. Edgington, P. McCabe, E. Pidcock, G.P. Shields, R. Taylor, M. Towler, J.v.d. Streek, J. Appl. Crystallogr. 39 (2006) 453–457.
[53] K. Nakamaru, Bull. Chem. Soc. Jpn. 55 (1982) 1639–1640.
[54] S.J. Bruce, I. Tavazzi, V.r. Parisod, S. Rezzi, S. Kochhar, P.A. Guy, Anal. Chem. 81 (2009) 3285–3296.
[55] M. Kozlowska, P. Rodziewicz, D.M. Brus, J. Breczko, K. Brzezinski, Acta Crystallogr. Sect. Sect. E: Struct. Rep. 68 (2012) m1414–m1415 Online.
[56] D.C. Craig, M.L. Scudder, W.-A. McHale, H.A. Goodwin, Aust. J. Chem. 51 (1998) 1131–1140.
[57] M.L. Scudder, D.C. Craig, H.A. Goodwin, CrystEngComm 7 (2005) 642–649.
[58] A.G. Walstrom, M. Pink, X. Yang, K.G. Caulton, Dalton Trans. (2009) 6001–6006.
[59] S. Pyo, E. Pérez-Cordero, S.G. Bott, L. Echegoyen, Inorg. Chem. 38 (1999) 3337–3343.
[60] C.A. Tovee, C.A. Kilner, J.A. Thomas, M.A. Halcrow, CrystEngComm 11 (2009) 2069–2077.
[61] C. Femoni, M.C. Iapalucci, G. Longoni, T. Lovato, S. Stagni, S. Zacchini, Inorg. Chem. 49 (2010) 5992–6004.
[62] K. Lashgari, M. Kritikos, R. Norrestam, T. Norrby, Acta Crystallographica Section C 55 (1999) 64–67.
[63] C.-C. Lin, P. Wang, L. Jin, H.-H. Li, S.-K. Lin, Z.-R. Chen, J. Clust. Sci. 26 (2015) 1011–1022.
[64] C.R. Groom, I.J. Bruno, M.P. Lightfoot, S.C. Ward, Acta Crystallographica section B: structural science, Crystal Engineering and Materials 72 (2016) 171–179.
[65] M.L. Scudder, H.A. Goodwin, I.G. Dance, New J. Chem. 23 (1999) 695–705.
[66] M. Stone, G. Crosby, Chem. Phys. Lett. 79 (1981) 169–173.
[67] M. Beley, J.-P. Collin, J.-P. Sauvage, H. Sugihara, F. Heisel, A. Miehé, J. Chem. Soc. Dalton Trans. (1991) 3157–3159.
[68] M. Maestri, N. Armaroli, V. Balzani, E.C. Constable, A.M.C. Thompson, Inorg. Chem. 34 (1995) 2759–2767.
[69] J.P. Collin, S. Guillerez, J.P. Sauvage, F. Barigelletti, L. De Cola, L. Flamigni, V. Balzani, Inorg. Chem. 30 (1991) 4230–4238.
[70] V. Pierroz, T. Joshi, A. Leonidova, C. Mari, J. Schur, I. Ott, L. Spiccia, S. Ferrari, G. Gasser, J. Am. Chem. Soc. 134 (2012) 20376–20387.
[71] J. Karges, P. Goldner, G. Gasser, Inorganics 7 (2019) 4.
[72] R. Bonnett, G. Martınez, Tetrahedron 57 (2001) 9513–9547.
[73] T.S. Mang, T.J. Dougherty, W.R. Potter, D.G. Boyle, S. Somer, J. Moan, Photochem. Photobiol. 45 (1987) 501–506.
[74] X. Zhang, M.A. Rodgers, J. Phys. Chem. 99 (1995) 12797–12803.
[75] M. Ericson, S. Grapengiesser, F. Gudmundson, A. Wennberg, O. Larkö, J. Moan, A. Rosen, Lasers Med. Sci. 18 (2003) 56–62.
[76] P. Zhang, L. Pei, Y. Chen, W. Xu, Q. Lin, J. Wang, J. Wu, Y. Shen, L. Ji, H. Chao, Chem Eur J 19 (2013) 15494–15503.
[77] J.-W. Liang, Y. Wang, K.-J. Du, G.-Y. Li, R.-L. Guan, L.-N. Ji, H. Chao, J. Inorg. Biochem. 141 (2014) 17–27.